Nucleon momentum distributions from inclusive electron scattering with superscaling analysis

Tongqi Liang [1], Zhongzhou Ren,[1,2,*] Dong Bai [1], and Jian Liu [3,4,5,†]

[1]*School of Physics Science and Engineering, Tongji University, Shanghai 200092, China*

[2]*Key Laboratory of Advanced Micro-Structure Materials, Ministry of Education, Shanghai 200092, China*

[3]*College of Science, China University of Petroleum (East China), Qingdao 266580, China*

[4]*Laboratory of High Precision Nuclear Spectroscopy, Insititute of Modern Physics, Chinese Academy of Sciences, Lanzhou 730000, China*

[5]*Guangxi Key Laboratory of Nuclear Physics and Nuclear Technology, Guangxi Normal University, Guilin 541004, China*

Nucleon momentum distributions are crucial windows to probe nuclear structures. They provide valuable information not only on mean-field structures but also on short-range correlations. The y scaling analysis generally serves as a tool to extract the nucleon momentum distribution from inclusive quasielastic electron cross sections. In this paper, we report new nucleon momentum distributions for deuteron, ^{3,4}He, ^{9}Be, and ^{12}C, extracted, based on ψ' scaling, directly from the latest high-precision experimental data. It is found that, for deuteron, ^{3,4}He, ^{9}Be, and ^{12}C, the ψ'-scaling method provides reasonable results in agreement with state-of-the-art *ab initio* calculations up to 3.5 fm^{-1}. These new nucleon momentum distributions can be helpful references for future studies of nuclear structures.

I. INTRODUCTION

Electron scattering is one of the most fruitful methods to investigate the physical properties of the nucleus [1]. Over the past several decades, elastic electron scattering has provided substantial nuclear information, such as charge density distributions [2–5] and neutron distributions [6,7]. Much effort has also gone into electron scattering at higher energy and momentum transfers, where quasielastic scattering starts to dominate the cross sections [8]. In the quasielastic scattering region, cross sections contain the elaborate information on nucleon momentum distributions. For instance, in Ref. [9] the cluster structure of nuclei is investigated in the momentum space by using the quasielastic electron scattering.

Nucleon momentum distributions are important quantities in nuclear physics, giving valuable information on both mean-field (MF) structures and short-range correlations [10]. In MF models, the individual nucleons are assumed to move in an average potential sourced by the other nucleons. They give a good description of low-momentum parts of nucleon momentum distributions. However, the MF models generally do not give a proper account of high-momentum tails of nucleon momentum distributions caused by short-range correlations [11–16]. This problem attracts lots of attention in recent years. See, e.g., Refs. [17–21] for representative experimental progress. Various theoretical calculations have been carried out to study high-momentum tails with realistic nuclear potentials, such as quantum Monte Carlo (QMC) [22], nuclear contact theory [23], no core shell model [24], hyperspherical

harmonics method [25], and antisymmetrized molecular dynamics [26]. In order to confront these theoretical calculations with experiments, it is important to extract from experimental data of cross sections the nucleon momentum distributions for different nuclei. This could be done by analyzing, e.g., inclusive electron scattering data in the quasielastic region [11,14,27,28].

Scaling is a powerful tool to study inclusive electron scattering in the quasielastic region [1,29–31]. Within the framework of the plane wave impulse approximation (PWIA), the inclusive electron cross section could be expressed as a product of the single-nucleon cross section and a specific function [30], the scaling function, that depends on the properties of the target nucleus and, as shown in Sec. II, is generally a function of two kinematic variables. In the limit of large momentum transfers this function scales and becomes a function of only one kinematic variable, the scaling variable.

Various scaling laws have been proposed in the literature for inclusive electron scattering, such as Y scaling [29], y scaling [34], y_{CW} scaling [35], ψ scaling [32], and ψ' scaling [33]. The scaling variable $Y = Y(q, \omega)$ was first introduced by West in the 1970s [29]. Later on, as an alternative to Y, the scaling variable y was proposed and widely used to analyze the inclusive electron scattering. By utilizing y scaling and evaluating the excitation energy of the recoil nuclei, Ciofi degli Atti *et al.* extracted the nucleon momentum distributions in few-body systems, complex nuclei, and nuclear matter [34]. Finally in 1999, Ciofi degli Atti and West proposed the scaling variable y_{CW}, which effectively reflects the excitation energy [35]. Among Y, y, and y_{CW}, we focus on the discussion of y scaling in this paper.

Motivated by the relativistic Fermi gas (RFG) model, ψ scaling and its improved version named as ψ' scaling can

*zren@tongji.edu.cn

†liujian@upc.edu.cn

naturally incorporate the excited states of the recoil nuclei [33]. ψ' scaling has been used to study inclusive electron scattering from ^{12}C, reproducing both the quasielastic peak and the $\Delta(1232)$ region [9,36]. Recently, it has also been generalized to study neutrino- and antineutrino-nucleus reactions [37–39]. In Ref. [40], it is mentioned that ψ' scaling could be used to extract nucleon momentum distributions. This idea, however, has not been explored systematically for different nuclei in combination with experimental data. We try to fill this gap by extracting and analyzing nucleon momentum distributions based on ψ' scaling and the latest high-precision experimental data.

The rest parts are organized as follows. In Sec. II, we review y scaling and ψ' scaling briefly. In Sec. III, we extract ψ' scaling functions and nucleon momentum distributions from the latest high-precision experimental data for different nuclei and compare the results with the y-scaling extractions [34] and the state-of-the-art QMC results [22,41]. Explicitly, we extract nucleon momentum distributions for deuteron, ^{3}He, ^{4}He, ^{9}Be, and ^{12}C, among which the nucleon momentum distribution of ^{9}Be has not been extracted from the inclusive cross sections in previous studies as far as we know. Finally, the summary and conclusions are given in Sec. IV.

II. THEORETICAL FRAMEWORK

PWIA plays an important role in establishing the theoretical formalism for scaling [30]. It assumes that the electron interacts only with one nucleon in the nucleus at one time and the interacting nucleon is emitted without interacting with the residual nucleus. Within the framework of the PWIA, the double differential cross section could be organized into the product of the single-nucleon cross section σ_{eN} and a function $F[Q^2, z(q, \omega)]$ for inclusive (e, e') scattering in the quasielastic region [30]

$$\frac{d^2\sigma}{d\Omega d\omega} = \tilde{\sigma}_{eN}(q, \omega; k, \varepsilon) \times F[Q^2, z(q, \omega)], \qquad (1)$$

where Ω is the solid angle of the outgoing electron, q is the electron momentum transfer, ω is the electron energy transfer, k is the nucleon momentum, ε is the excitation energy of the residual $A - 1$ system, $Q^2 = q^2 - \omega^2$ is the four-momentum transfer squared, and $z(q, \omega)$ is the so-called scaling variable. Various choices are available in the literature for the scaling variable z. Two of them are reviewed briefly in the following subsections.

A. y scaling

One popular choice for the scaling variable $z(q, \omega)$ is given by the kinematic variable y satisfying [30]

$$\omega + M_A = \left[m_N^2 + (q + y)^2\right]^{1/2} + \left[M_{A-1}^2 + y^2\right]^{1/2}, \qquad (2)$$

where M_A, m_N, and M_{A-1} are the masses of the target nucleus, the knocked-out nucleon, and the recoil nucleus $A - 1$, respectively. Physically, y could be identified as the lowest longitudinal momentum of the knocked-out nucleon along the direction of $\mathbf{q}$ when $\varepsilon = 0$. Noticeably, it is M_{A-1} that is used in defining the scaling variable y, which means that the recoil

nucleus $A - 1$ is assumed to be in its ground state. In other words, we do not consider the inner excitation of the recoil nucleus.

For high Q^2, $F(Q^2, y)$ becomes independent of Q^2 and is reduced to the one-variable function $F(y)$ which is also known as the y scaling function [30]. Then, the double differential cross section in Eq. (1) becomes [30]

$$\frac{d^2\sigma}{d\Omega d\omega} = \tilde{\sigma}_{eN}(q, y; k = |y|, \varepsilon = 0) \times F(y), \qquad (3)$$

where $\tilde{\sigma}_{eN}$ is computed by Eq. (13) in Ref. [42]. Following Ref. [34], the nucleon momentum distribution $n(k)$ can be extracted from the y scaling function by

$$n(k) = -\frac{1}{2\pi y}\left[\frac{dF(y)}{dy}\right]_{|y|=k}. \qquad (4)$$

In the following, the method using Eqs. (2) and (4), where the excitation of the recoil nucleus is ignored, is referred to as y scaling without the excitation energy.

B. ψ' scaling

Another popular choice for the scaling variable $z(q, \omega)$ is given by [33]

$$\psi' \equiv \frac{1}{\sqrt{\xi_F}} \frac{\lambda' - \tau'}{\sqrt{(1 + \lambda')\tau' + \kappa\sqrt{\tau'(\tau' + 1)}}} \qquad (5)$$

with $\kappa \equiv q/2m_N$, $\lambda' \equiv \omega/2m_N - E_{\text{shift}}/2m_N$, $\tau' = \kappa^2 - \lambda'^2$, $\eta_F \equiv k_F/m_N$, $\xi_F \equiv \sqrt{1 + \eta_F^2} - 1$, and k_F being the Fermi momentum. The above definition of ψ' is motivated within the framework of the relativistic Fermi gas (RFG) model, which considers explicitly the possible excitation of the recoil nucleus [43]. Besides, both the scattering process and the bound nucleon dynamics are handled with the relativistic kinematics. In the definition of λ', an extra empirical parameter E_{shift} is introduced to simulate the impact of nucleon separation energy $E_s = M_{A-1} + m_N - M_A$, which is found to be important in modeling the quasielastic peak. When $E_{\text{shift}} = 0$, the variable ψ' in Eq. (5) is reduced to the variable ψ. With the scaling variable ψ', the double differential cross section may be given by [33]

$$\frac{d^2\sigma}{d\Omega d\omega} \cong \sigma_M\left[\frac{\kappa}{2\tau}v_L\tilde{G}_E^2 + \frac{\tau}{\kappa}v_T\tilde{G}_M^2\right] \times F(Q^2, \psi'), \qquad (6)$$

where σ_M is the Mott cross section, $v_{L(T)}$ is the electron longitudinal (transverse) kinematical factor, and $\tilde{G}_{E(M)}^2 = ZG_{E(M)p}^2 + NG_{E(M)n}^2$ is the combining of the Sachs form factors.

For high Q^2, $F(Q^2, \psi')$ becomes independent of Q^2. In this region, we can define the ψ' scaling function $f(\psi')$ as

$$f(\psi') = k_F \times F(\psi'). \qquad (7)$$

Inspired by Eq. (4), the nucleon momentum distribution $f(\psi')$ could be given by

$$n(k) = -\frac{1}{2\pi y k_F}\left[\frac{df(\psi')}{d(k_F\psi')}\right]_{|y|=k}, \qquad (8)$$

with $\psi' \approx \frac{y}{k_F} + \frac{\eta_F y^2}{2k_F^2}\sqrt{1 + \frac{m_N^2}{q^2}}$ [33].

III. NUMERICAL RESULTS

Nucleon momentum distributions extracted from experimental data are fundamentally important in validating theoretical models of nuclear structures. As mentioned in the Introduction, y scaling is often adopted to extract nucleon momentum distributions from experimental inclusive electron cross sections. In this paper, we extract new nucleon momentum distributions from the latest high-precision experimental data by using the ψ'-scaling method given in Sec. II B and compare them with the QMC calculations. Deuteron, ^{3}He, ^{4}He, ^{9}Be, and ^{12}C are taken as examples, with the inclusive electron cross sections from Refs. [8,44,45]. As shown in Eq. (5), the Fermi momentum k_F and energy shift E_{shift} are needed for defining the ψ' scaling variable. In the following calculations, the Fermi momenta are taken to be $k_F = 55, 140, 200, 195,$ and 228 MeV/c for deuteron, ^{3}He, ^{4}He, ^{9}Be, and ^{12}C, while $E_{\text{shift}} = 0, 15, 15, 15,$ and 20 MeV.

In Fig. 1, we re-evaluate ψ' scaling functions for deuteron, ^{3}He, ^{4}He, ^{9}Be, and ^{12}C, which act as the theoretical foundation for our extraction of nucleon momentum distributions from experimental inclusive cross section data. It is also very interesting to add the error bars for the extractions. Error propagation is a complicated task in both physical and computational areas. In this paper, the statistical errors of experimental data are propagated by means of Monte Carlo simulations [46]. We assume that experimental data are independent from each other and follow Gaussian distributions centered around the measured values with a width given by the error. Drawing random samples from these distributions, one can get a collection of scaling functions and nucleon momentum distributions, which are used to determine the errors. In our study, 50000 samples are generated for each scaling function and nucleon momentum distribution and there is no obvious change in final results when we increase the sample numbers.

Compared with previous studies in, e.g., Ref. [34], our present analysis is featured by the usage of the latest high-precision experimental data reported in Refs. [8,44,45]. To our best knowledge, such a study has not been reported in a public way. Figure 1(a) shows the ψ' scaling functions $f(\psi')$ for deuteron, which are extracted by using Eq. (7) from four sets of electron scattering data with the electron incident energies and scattering angles $(E, \theta) = (4.045 \text{ GeV}, 55°)$, $(5.766 \text{ GeV}, 18°)$, $(5.766 \text{ GeV}, 22°)$, and $(5.766 \text{ GeV}, 26°)$ [8,44,45]. For each data set, the Q^2 value is measured at the corresponding quasielastic peak. It is straightforward to see the celebrating independence of $f(\psi')$ on Q^2 in the scaling region $\psi' < 0$. Figure 1(b) shows the ψ' scaling functions for ^{3}He, ^{4}He, ^{9}Be, and ^{12}C at $(E, \theta) = (5.766 \text{ GeV}, 32°)$. Once again, in the scaling region $\psi' < 0$, a universal curve is observed for different nuclei. For $\psi' > 0$, ψ' scaling is, however, badly violated as shown in Figs. 1(a) and 1(b), as the $\Delta(1232)$ resonance, deep inelastic scattering, and other processes beyond quasielastic scattering contribute significantly to inclusive cross sections in this region.

A. Deuteron

As shown in Sec. II B, the nucleon momentum distribution $n(k)$ of the deuteron can be extracted from the ψ' scaling function $f(\psi')$ within the framework of PWIA by using
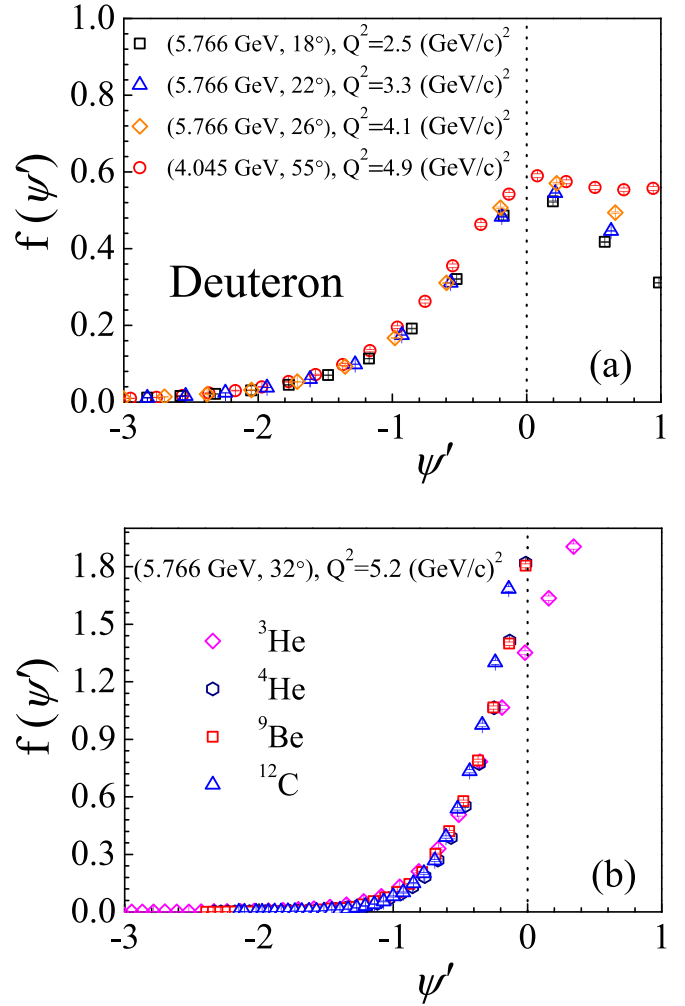

FIG. 1. (a) The ψ' scaling functions $f(\psi')$ for deuteron obtained from the latest inclusive electron scattering data with the electron incident energies and scattering angles given by $(E, \theta) = (4.045 \text{ GeV}, 55°)$, $(5.766 \text{ GeV}, 18°)$, $(5.766 \text{ GeV}, 22°)$, and $(5.766 \text{ GeV}, 26°)$, separately [8,44,45]. (b) The ψ' scaling functions $f(\psi')$ for ^{3}He, ^{4}He, ^{9}Be, and ^{12}C from the latest inclusive electron scattering data with the electron incident energy and scattering angle given by $(E, \theta) = (5.766 \text{ GeV}, 32°)$ [8,44]. The error bars of $f(\psi')$ are also shown in the figure.

Eq. (8). The numerical results are shown in Fig. 2 for four sets of electron incident energies and scattering angles. For comparison, we also plot on the same figures the results from y scaling without the excitation energy given by Eq. (4) and the QMC results [22,41] with three different realistic interactions including AV18 [47], NV2-Ia, and NV2-IIa [48,49], along with the numerical results reported in Ref. [34] which are based on the y-scaling method and include the excitation energy.

In Fig. 2, it is straightforward to see that the deuteron nucleon momentum distributions $n(k)$ given by ψ' scaling coincide perfectly with the results of y scaling without the excitation energy, QMC, and Ref. [34]. Moreover, ψ' scaling is found to give almost the same nucleon momentum distributions for different electron incident energies and scattering
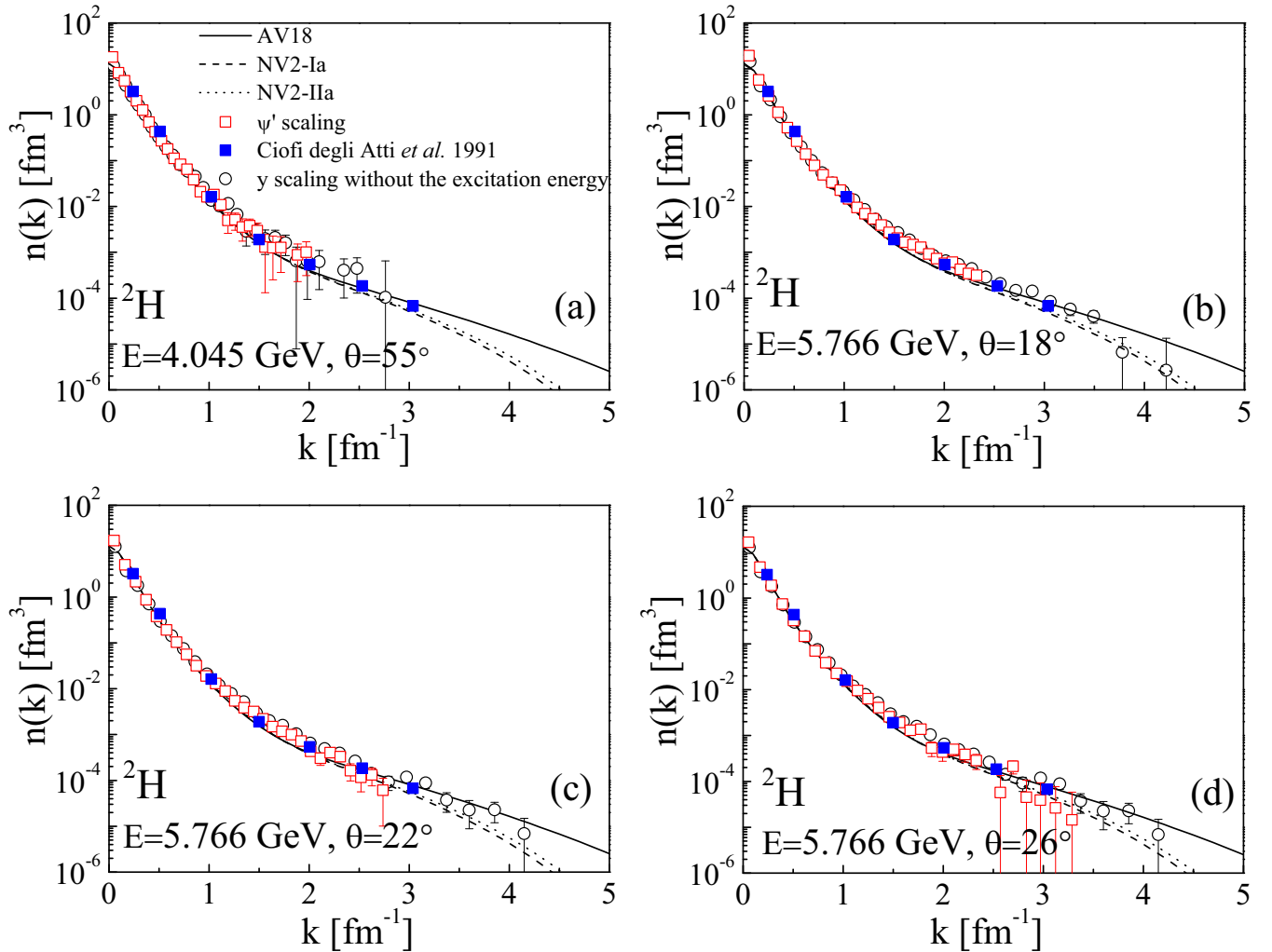
FIG. 2. Nucleon momentum distributions of deuteron extracted from the latest inclusive electron scattering data with the electron incident energies and scattering angles given by $(E, \theta) = (4.045 \text{ GeV}, 55°)$, $(5.766 \text{ GeV}, 18°)$, $(5.766 \text{ GeV}, 22°)$, and $(5.766 \text{ GeV}, 26°)$, separately [8,44,45]. The red squares correspond to our results based on ψ' scaling. The results from y scaling without the excitation energy (circles), the results from Ciofi degli Atti *et al.* 1991 [34] (blue squares), and the theoretical results from QMC with different realistic *NN* interactions (AV18, NV2-Ia, and NV2-IIa) [22,41] (solid, dashed, and dotted lines) are also shown for comparison. The error bars of the extractions are also shown in the figure.

angles as shown by the four panels of Fig. 2. This is consistent with the expectation that nucleon momentum distributions are intrinsic properties of nuclei. They should not be affected by different experimental setups. These results provide nontrivial evidence on the reliability of our extractions of nucleon momentum distributions based on ψ' scaling, which encourages us to extract nucleon momentum distributions from inclusive electron scattering data for more nuclei.

B. ³He, ⁴He, ⁹Be, and ¹²C

In Fig. 3, we show the nucleon momentum distributions $n(k)$ up to 3.5 fm⁻¹ for ³He, ⁴He, ⁹Be, and ¹²C, extracted from inclusive electron scattering data with the help of the ψ'-scaling method. Noticeably, the nucleon momentum distribution of ⁹Be is extracted from the experimental cross sections for the first time. The inclusive cross section data are taken for the same kinematic parameter with the elec-

tron incident energy and scattering angle given by $(E, \theta) = (5.766 \text{ GeV}, 32°)$ [44]. In the same figure, we also plot the results of y scaling without the excitation energy, Ref. [34] (without ⁹Be), and the QMC calculations [22,41] with the two-nucleon potential AV18 and three-nucleon potential UX [50] for comparison.

It is straightforward to see that these three methods of $n(k)$ extractions are generally consistent with the QMC results from low-momentum regions to high-momentum regions up to 3.5 fm⁻¹. In the region $k < 1.5$ fm⁻¹ where the effects of the excitation energy are not obvious, three methods give the approximately same results. In the region $1.5 < k < 2.3$ fm⁻¹ where the change of the slope of $n(k)$ generated by the crossing of the s and p shell model distributions is active, the ψ'-scaling results slightly overestimate the QMC calculations and the results reported in Ref. [34] slightly underestimate the QMC calculations. The results of the ψ'-scaling method and those in Ref. [34] respectively provide the upper and
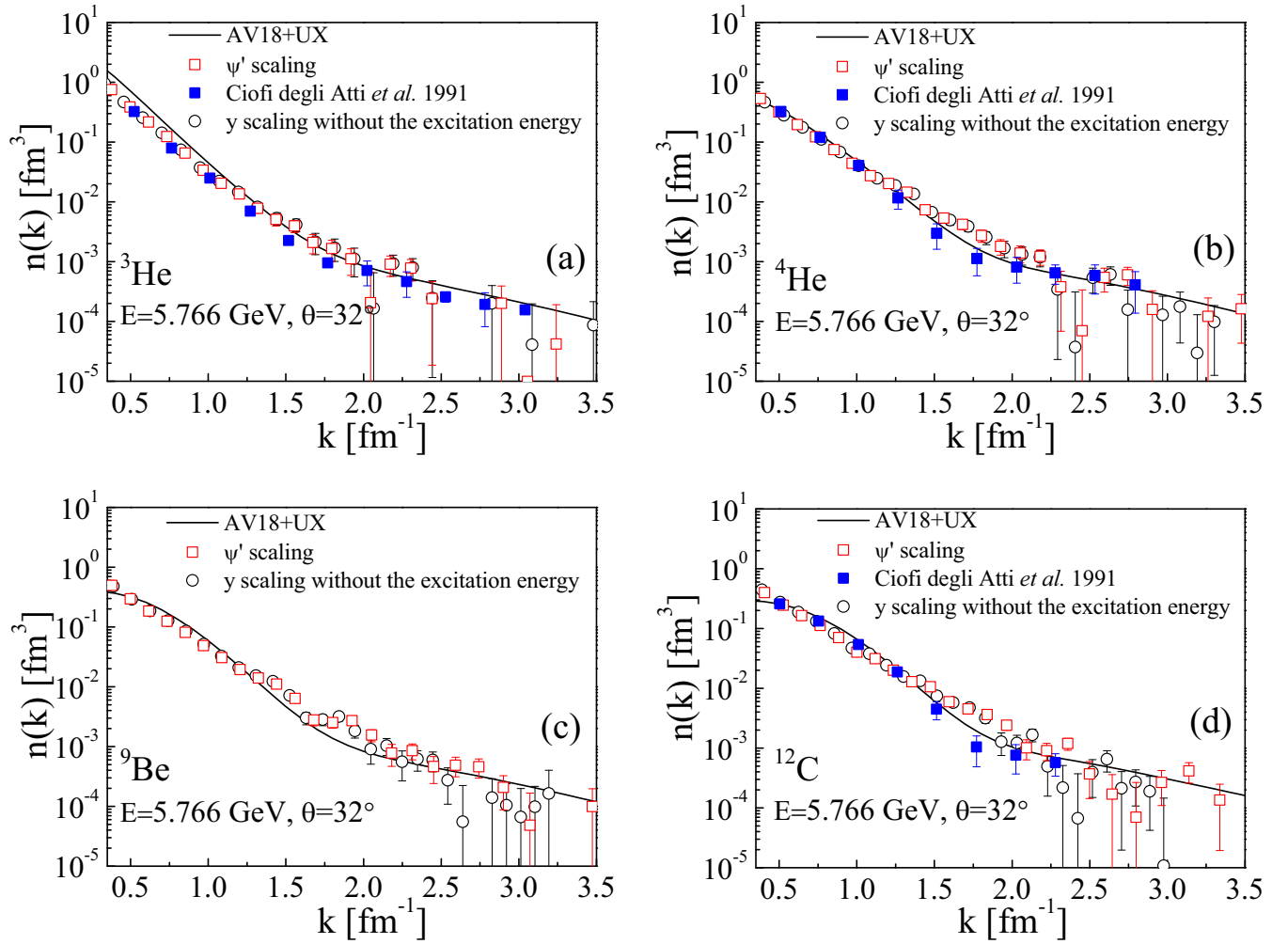
FIG. 3. Nucleon momentum distributions of ^{3}He, ^{4}He, ^{9}Be, and ^{12}C extracted from the latest inclusive electron scattering data with the electron incident energies and scattering angles given by $(E, \theta) = (5.766 \text{ GeV}, 32°)$ [44]. The red squares correspond to our new results based on ψ' scaling. The results from y scaling without the excitation energy (circles), the results from Ciofi degli Atti *et al.* 1991 [34] (blue squares), and the theoretical results from QMC with the realistic AV18 + UX interactions [22,41] (lines) are also shown for comparison. The error bars of the extractions are also shown in the figure.

lower limits of the nucleon momentum distribution in this region. Focusing on the high-momentum region ($2.5 < k < 3.5 \text{ fm}^{-1}$), the nucleon momentum distributions of ^{9}Be and ^{12}C given by y scaling without the excitation energy slightly undershoot the QMC results for the absence of the excitation energy, which is considered in ψ' scaling and Ref. [34]. The ψ' scaling analysis gives more reliable extractions of high-momentum tails of nucleon momentum distributions, especially for ^{4}He and ^{12}C, as the nucleon momentum distributions of these two nuclei given by Ref. [34] in this region are missing. This suggests that our results could be helpful references for future studies of high-momentum tails and short-range correlations in these nuclei. By comparing the ψ'-scaling extractions with reliable theoretical expectations and results in Ref. [34], it is fair to say that the ψ'-scaling method can reproduce many important features of mean-field and short-range structures.

We remark that the nucleon momentum distributions are extracted by the scaling method in the framework of the PWIA, without considering meson-exchange currents (MEC)

rescattering and final-state interactions (FSI). These contributions can lead to scaling violations and influence the extracted nucleon momentum distribution. It is interesting to consider the contributions of MEC and FSI to the experimental cross sections. However, it is not trivial to calculate these two effects explicitly. For the experimental data with high momentum transfers used in this paper, the influences of MEC and FSI are not significant in the region below the quasielastic peak (i.e., $\psi' < 0$) [51,52]. Scaling limits are reached within the impulse approximation and the reasonable nucleon momentum distributions are extracted. An evaluation of MEC and FSI will be performed in the following studies.

IV. SUMMARY AND CONCLUSIONS

In summary, we report new nucleon momentum distributions of the deuteron, ^{3}He, ^{4}He, ^{9}Be, and ^{12}C extracted from various inclusive electron scattering data by using ψ' scaling. The new results are consistent with the state-of-the-art QMC calculations with realistic nuclear interactions. In the

high-momentum region around 3.5 fm^{-1}, where the nucleon momentum distributions correspond to short-range correlations and are not extracted in Ref. [34], it is found that the ψ'-scaling method provides reasonable results for ^{3,4}He, ^{9}Be, and ^{12}C. Our new results are helpful references for experimental and theoretical studies on short-range correlations in the future. It may also help to understand the implications of short-range correlations on neutron star properties [53,54]. Moreover, it can provide useful guides for the new Electron-Ion Collider in China [16].

[1] B. Foris and C. N. Papanicolas, Annu. Rev. Nucl. Part. Sci. **37**, 133 (1987).

[2] T. Suda *et al.*, Phys. Rev. Lett. **102**, 102501 (2009).

[3] K. Tsukada, A. Enokizono, T. Ohnishi, K. Adachi, T. Fujita, M. Hara, M. Hori, T. Hori, S. Ichikawa, K. Kurita, K. Matsuda, T. Suda, T. Tamae, M. Togasaki, M. Wakasugi, M. Watanabe, and K. Yamada, Phys. Rev. Lett. **118**, 262501 (2017).

[4] J. Liu, C. Xu, and Z. Ren, Phys. Rev. C **95**, 044318 (2017).

[5] T. Liang, J. Liu, Z. Ren, C. Xu, and S. Wang, Phys. Rev. C **98**, 044310 (2018).

[6] P. Sarriguren, D. Merino, O. Moreno, E. Moya de Guerra, D. N. Kadrev, A. N. Antonov, and M. K. Gaidarov, Phys. Rev. C **99**, 034325 (2019).

[7] B. Hernández, P. Sarriguren, O. Moreno, E. Moya de Guerra, D. N. Kadrev, and A. N. Antonov, Phys. Rev. C **103**, 014303 (2021).

[8] N. Fomin *et al.*, Phys. Rev. Lett. **108**, 092502 (2012).

[9] L. Wang, J. Liu, R. Wang, M. Lyu, C. Xu, and Z. Ren, Phys. Rev. C **103**, 054307 (2021).

[10] R. Silver and P. Sokol, *Momentum Distributions* (Plenum, New York, 1989).

[11] C. Ciofi degli Atti, Phys. Rep. **590**, 1 (2015).

[12] A. N. Antonov, P. E. Hodgson, and I. Z. Petkov, *Nucleon Correlations in Nuclei* (Springer-Verlag, Berlin, 1993).

[13] O. Hen, G. A. Miller, E. Piasetzky, and L. B. Weinstein, Rev. Mod. Phys. **89**, 045002 (2017).

[14] N. Fomin, D. Higinbotham, M. Sargsian, and P. Solvignon, Annu. Rev. Nucl. Part. Sci. **67**, 129 (2017).

[15] X. Wang, Q. Niu, J. Zhang, M. Lyu, J. Liu, C. Xu, and Z. Ren, Sci. China Phys. Mech. Astron. **64**, 292011 (2021).

[16] D. P. Anderle *et al.*, Front. Phys. **16**, 64701 (2021).

[17] M. Duer *et al.* (CLAS Collaboration), Nature (London) **560**, 617 (2018).

[18] O. Hen *et al.*, Science **346**, 614 (2014).

[19] B. Schmookler *et al.* (CLAS Collaboration), Nature (London) **566**, 354 (2019).

[20] A. Schmidt *et al.* (CLAS Collaboration), Nature (London) **578**, 540 (2020).

[21] R. Cruz-Torres *et al.*, Nat. Phys. **17**, 306 (2021).

[22] R. B. Wiringa, R. Schiavilla, S. C. Pieper, and J. Carlson, Phys. Rev. C **89**, 024305 (2014).

[23] R. Weiss, B. Bazak, and N. Barnea, Phys. Rev. Lett. **114**, 012501 (2015).

[24] T. Neff, H. Feldmeier, and W. Horiuchi, Phys. Rev. C **92**, 024003 (2015).

[25] L. E. Marcucci, F. Sammarruca, M. Viviani, and R. Machleidt, Phys. Rev. C **99**, 034003 (2019).

[26] M. Lyu, T. Myo, H. Toki, H. Horiuchi, C. Xu, and N. Wan, Phys. Lett. B **805**, 135421 (2020).

[27] Q. Niu, J. Liu, Y. Guo, C. Xu, M. Lyu, and Z. Ren, Phys. Rev. C **105**, L051602 (2022).

[28] O. Benhar, D. Day, and I. Sick, Rev. Mod. Phys. **80**, 189 (2008).

[29] G. B. West, Phys. Rep. **18**, 263 (1975).

[30] D. B. Day, J. S. McCarthy, T. W. Donnelly, and I. Sick, Annu. Rev. Nucl. Part. Sci. **40**, 357 (1990).

[31] J. D. Walecka, *Electron Scattering for Nuclear and Nucleon Structure* (Cambridge University Press, Cambridge, 2001).

[32] W. M. Alberico, A. Molinari, T. W. Donnelly, E. L. Kronenberg, and J. W. Van Order, Phys. Rev. C **38**, 1801 (1988).

[33] T. W. Donnelly and I. Sick, Phys. Rev. Lett. **82**, 3212 (1999); Phys. Rev. C **60**, 065502 (1999).

[34] C. Ciof idegli Atti, E. Pace, and G. Salme, Phys. Rev. C **43**, 1155 (1991).

[35] C. Ciofi degli Atti and G. B. West, Phys. Lett. B **458**, 447 (1999).

[36] A. N. Antonov, M. V. Ivanov, M. K. Gaidarov, E. Moya de Guerra, J. A. Caballero, M. B. Barbaro, J. M. Udias, and P. Sarriguren, Phys. Rev. C **74**, 054603 (2006).

[37] J. E. Amaro, M. B. Barbaro, J. A. Caballero, and T. W. Donnelly, Phys. Rev. Lett. **98**, 242501 (2007).

[38] G. D. Megias, J. E. Amaro, M. B. Barbaro, J. A. Caballero, and T. W. Donnelly, Phys. Lett. B **725**, 170 (2013).

[39] G. D. Megias, S. Bolognesi, M. B. Barbaro, and E. Tomasi-Gustafsson, Phys. Rev. C **101**, 025501 (2020).

[40] J. A. Caballero, M. B. Barbaro, A. N. Antonov, M. V. Ivanov, and T. W. Donnelly, Phys. Rev. C **81**, 055502 (2010).

[41] R. B. Wirgina, Single-Nucleon Momentum Distributions, https://www.phy.anl.gov/theory/research/momenta/

[42] T. De Forest, Jr., Nucl. Phys. A **392**, 232 (1983).

[43] R. Cenni, T. W. Donnelly, and A. Molinari, Phys. Rev. C **56**, 276 (1997).

[44] O. Benhar, D. Day, and I. Sick, arXiv:nucl-ex/0603032 [nucl-ex].

[45] J. Arrington *et al.*, Phys. Rev. Lett. **82**, 2056 (1999).

[46] J. Zhang, WIREs Comput. Stat. **13**, e1539 (2021).

[47] R. B. Wiringa, V. G. J. Stoks, and R. Schiavilla, Phys. Rev. C **51**, 38 (1995).

[48] M. Piarulli, L. Girlanda, R. Schiavilla, R. N. Pérez, J. E. Amaro, and E. Ruiz Arriola, Phys. Rev. C **91**, 024003 (2015).

[49] M. Piarulli and I. Tews, Front. Phys. **7**, 245 (2020).

[50] S. C. Pieper, V. R. Pandharipande, R. B. Wiringa, and J. Carlson, Phys. Rev. C **64**, 014001 (2001).

[51] A. De Pace, M. Nardi, W. M. Alberico, T. W. Donnelly, and A. Molinari, Nucl. Phys. A **741**, 249 (2004).

[52] D. Faralli, C. Ciofi degli Atti, and G. West, arXiv:nucl-th/9910065 [nucl-th].

[53] L. A. Souza, M. Dutra, C. H. Lenzi, and O. Lourenço, Phys. Rev. C **101**, 065202 (2020).

[54] H. Lu, Z. Ren, and D. Bai, Nucl. Phys. A **1011**, 122200 (2021).